Digest 2010, December 2010 1425-1444

Investigation of FRP Strengthening Design Rules for Insufficient RC Columns†

Okan ÖZCAN*
Barış BİNİCİ**
Güney ÖZCEBE***

ABSTRACT

Increasing the deformation capacities of code-incompliant RC columns by wrapping their potential plastic hinge regions with fiber-reinforced polymer (FRP) has become a rather popular strengthening technique in recent years. FRP design guidelines are included in the 7th chapter of the Turkish Earthquake Code (TEC-07) that became effective in 2007. This study intends to scrutinize the design approach of TEC-07 in light of the test results of 10 columns tested under axial load and cyclic displacement excursions at METU and the test results of 18 columns gathered from literature. After careful investigations, it was clearly seen that in TEC-07, the FRP wrapped column performance limits were over conservative and led to uneconomical designs. Two different design methods were developed. The first one is compatible with the current code procedure and the other is based on interstory drifts in order to obtain simpler and more economical FRP design in addition to its accuracy.

Keywords: *Columns, flexural behavior, CFRP confinement, Turkish Earthquake Code*

1. INTRODUCTION

The use of fiber reinforced polymer (FRP) materials in columns for strengthening and repair purposes has been widely utilized in recent years and many researchers demonstrated this technique as a practical method that can be used in buildings and bridge columns [1-10]. For the columns under seismic loading, FRP confinement permits to meet displacement demands without a significant increase in column's lateral strength. Thus, FRP wrapping can be implemented as a substantially efficient method in order to retrofit the plastic hinge regions of the columns having insufficient confinement. Among all retrofitting methods for the buildings with inadequate seismic performance, FRP wrapping method is an alternative economical and easy-to-implement retrofitting method to increase the deformation capacities of the columns having insufficient confinement. For this purpose, FRP design method to increase column ductility was introduced in Turkish

* Akdeniz University, Antalya, Turkey - ozcanok@gmail.com
** Middle East Technical University, Ankara, Turkey - binici@metu.edu.tr
*** Middle East Technical University, Ankara, Turkey - ozcebe@metu.edu.tr
† Published in Teknik Dergi Vol. 21, No. 4 October 2010, pp: 5219-5239

Earthquake Code (TEC07) [11]. The equations denoted below (Equations 1-4) enable the calculation of concrete strength and crushing strain according to the code.

$$f_{cc} = f_{cm}\left(1+\left(\frac{f_l}{f_{cm}}\right)\right) \geq 1.2 f_{cm} \tag{1}$$

$$\varepsilon_{cc} = 0.002\left(1+15\left(\frac{f_l}{f_{cm}}\right)^{0.75}\right) \tag{2}$$

$$f_l = \frac{\kappa_a \rho_f \varepsilon_f E_f}{2} \tag{3}$$

$$\kappa_a = 1 - \frac{(h-2r)^2 + (b-2r)^2}{3bh} \tag{4}$$

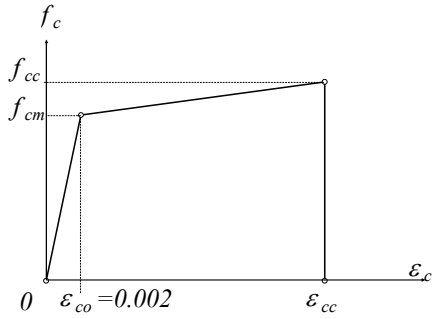

Figure 1. FRP confined concrete model indicated in the code

Herein, the parameters of f_l, κ_a, ρ_f, ε_f, E_f, f_{cm} denote FRP confinement pressure, shape efficiency coefficient, FRP volumetric ratio, FRP design rupture strain, FRP elasticity modulus and unconfined concrete compressive stress, respectively. In the third equation given above, ε_f value cannot be taken more than half of the rupture strain recommended by the manufacturer. According to TEC07, FRPs will not increase the column ductility if the increase in uniaxial compressive strength is less than 20%. For the analyses in which linear elastic method is used, in order to consider FRP retrofitted section as confined section, the crushing strain value that was stated in Equation 2 should exceed 0.018. If the linear

inelastic methods are used, the damage limits need to be determined by modeling the FRP confined concrete behavior under lateral pressure by bilinear stress strain relationship. This research intends to reexamine and to improve the design rules for ductility improvement in FRP confined columns in the light of experimental and analytical studies according to TEC07. The points of commencement of this study are the following observations related to FRP design rules denoted in TEC07:

1) The concrete strain limit introduced in Equation 2 may not represent realistic column damage levels since this equation was suggested using the experimental results of FRP confined columns under axial load alone.

2) The design rules should be examined in light of experimental results of columns subjected to combined and lateral loads. In this way, economical and safe designs can be ensured.

3) In the FRP design method of TEC07, a 20 percent absolute axial capacity gain for ductility improvement is recommended for the cross section analyses. Instead of such an approach, simple and sound design equations are needed for safe and economical designs.

An experimental and analytical study was, therefore, carried out to overcome the shortcomings of the present code requirements of FRP design. First, the column test results conducted at METU were summarized and specimen performances were predicted by using the design method indicated in TEC07. Afterwards, two different design methods were recommended based on METU test results and additional FRP confined column test results reported by other researchers. In the first method, an approach that depends on the determination of column drift levels (or chord rotations) is introduced; and in the second method, a code compatible approach that employs strain limits is recommended. Improved recommendations for future updates of the code are proposed based on the experimental and analytical results.

2. METU TESTS

The experimental study reported in this paper was conducted on near full-scale column models that emulate RC columns with code incompliant designs (widely spaced stirrups, 90-degree hooks and low compressive strength concrete) that can be encountered in this country and elsewhere. In this study, 3 references and 10 FRP confined flexural columns were tested and the effects of (a) the level of FRP confinement provided, (b) the level of axial load and (b) the longitudinal reinforcement ratio on column seismic performance were investigated. The properties of the test specimens are shown in Table 1. In the conducted tests, all columns were tested under constant axial load and reversed cyclic displacement excursions. Herein, for the column tests that comprised of 3 series, one as-built reference column that belonged to each test series was used. The reinforcement properties used for the columns and the test setup are shown in Figure 2.

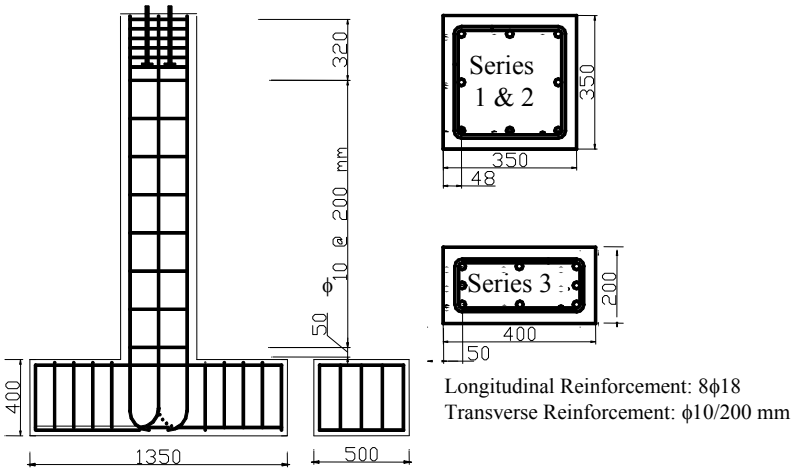

(a)

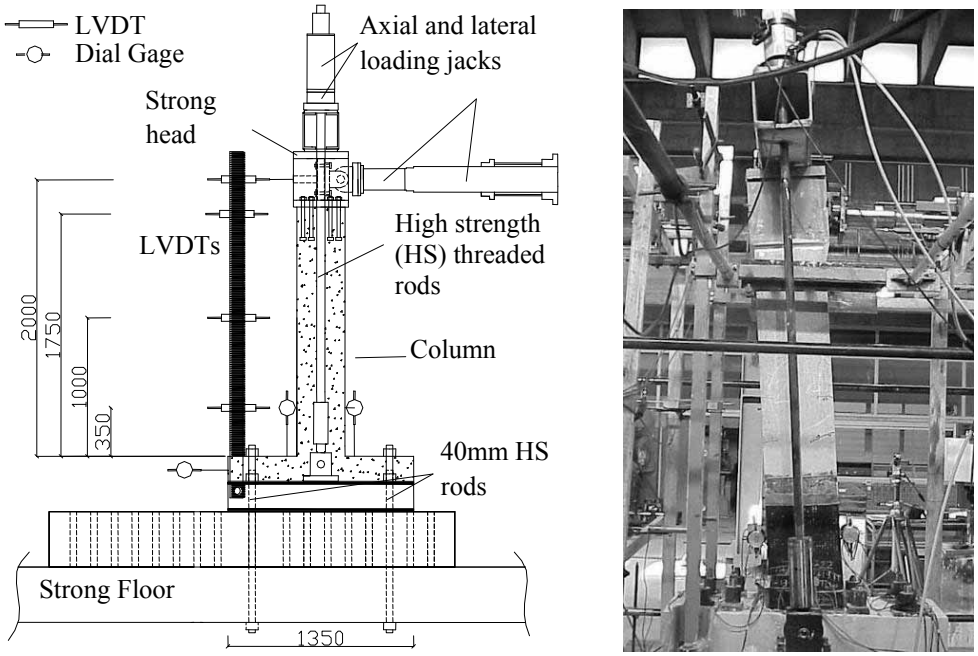

(b) (c)

Figure 2. (a) The properties of test specimens, (b) and (c) Test setup

Table 1. The properties of the test specimens

Series	Specimen	b	h	L	R	f_{cm}	A_s	κ_a	ρ	n*	ϕ	DR_u
		mm	*mm*	*mm*	*mm*	*MPa*	mm^2		*%*	*%*		*%*
	S-L-0-00	350	350	2000	-	14.0	2035.8	-	1.66	35	-	2.6
	S-L-1-00	350	350	2000	30	19.4	2035.8	0.542	1.66	27	0.091	4.9
Series 1	S-L-1-34	350	350	2000	30	14.0	2035.8	0.542	1.66	34	0.126	5.1
	S-L-2-00	350	350	2000	30	11.4	2035.8	0.542	1.66	40	0.309	6.3
	S-L-2-32	350	350	2000	30	15.6	2035.8	0.542	1.66	32	0.226	6.0
	S-H-0-00	350	350	2000	-	20.0	3041.1	-	2.48	27	-	3.3
Series 2	S-H-1-00	350	350	2000	30	20.0	3041.1	0.542	2.48	27	0.088	4.1
	S-HC-1-00	350	350	2000	10	22.0	3041.1	0.407	2.48	27	0.066	3.6
	R-NC-0-00	200	400	2000	-	12.0	2035.8	-	2.54	35	-	1.8
	R-HC-1-16P	200	400	2000	30	10.0	2035.8	0.755	2.54	35	0.322	6.1
Series 3	R-MC-1-8P	200	400	2000	30	10.5	2035.8	0.437	2.54	35	0.178	3.7
	R-MC-1-NP	200	400	2000	30	9.0	2035.8	0.437	2.54	35	0.207	3.9
	R-MC-1-16P	200	400	2000	30	15.0	2035.8	0.755	2.54	35	0.215	4.0

$$*n = \frac{N_{applied}}{N_0} = \frac{N_{applied}}{0.85 f_c' bh + A_s f_{sy}}$$

Note: κ_a, ρ, n and ϕ parameters denote shape efficiency coefficient, longitudinal reinforcement ratio, axial load ratio and FRP lateral confinement ratio (Equations 1-4). DR_u denotes the column drift ratio at which the column lateral strength dropped to 80% of capacity.

For the test specimens of the first series that are shown in Table 1, FRP confinement amount and concrete compressive strength were taken as the major parameters. Subsequently three column specimens were tested in order to examine the effect of longitudinal reinforcement ratio and corner rounding radius on column behavior. The parameters investigated for the remaining five specimens were designated to be column aspect ratio and FRP confinement amount. The lateral load (P) versus lateral deflection (Δ) curves and the important events such as column-stub interface cracking, FRP debonding, FRP rupture and reinforcement buckling that were observed during the tests are shown in Figures 3-5. All detailed observations related to test results are not repeated here since these observations were explained in detail in the previous studies [1, 14-16]. In the tests, it was determined that increasing the FRP amount enhanced the deformation capacities of columns significantly and consequently provided improved ductility levels. The parameter that is shown as the FRP confinement ratio (ϕ) in Table 1 is the ratio of lateral confinement pressure (f_l) to the concrete compressive strength (f_{cm}). The drift ratios (DR) were obtained by dividing the measured column tip deflection by the column height. Column ultimate drift capacity (DR_u) was obtained by dividing the column tip deflection corresponding to 20 percent decrease in strength to the column height. As can be seen in Figure 6, increasing the

FRP confinement ratio led to an increase in the column drift capacities (DR_u) for different longitudinal reinforcement ratios. On the other hand, as the longitudinal reinforcement ratio gradually increased from 1.6% to 2.5%, a reduced amount of increase in column drift capacities were observed. Considering the lateral drift ratios in Table 1, it can be seen that increasing the ratios of axial load and/or longitudinal reinforcement led to deterioration in column seismic performance. As can be seen in the test results, these three major parameters (ϕ: FRP confinement ratio, n: axial load ratio, ρ: longitudinal reinforcement ratio) have a significant influence on the deformation capability of flexural columns.

3. EVALUATION ACCORDING TO TEC07

In the evaluations, the bilinear stress strain relationship for FRP confined concrete described in TEC07 was used. The yield curvature (K_y) and corresponding moment (M_y) values were calculated by section analysis using the FRP confined concrete and steel models denoted in TEC07. The results are shown in Table 2. The yield deflection (Δ_y) and corresponding lateral load values (F_y) were determined by assuming that the yield curvature develops at the column base and linear curvature distribution along column height. In the calculations, the yield curvature was defined as the ratio of yield moment to the cracked concrete rigidity, i.e. M_y/E_cI_{cr}. The E_cI_{cr} value shown in Table 2 is the cracked concrete rigidity specified by the code and it was calculated by proportioning between 0.4EI and 0.8EI values since the axial load ratios in the tests varied between 10% and 40%. In the calculation of ultimate deflection (Δ_u) and corresponding lateral load (P_u), the ultimate curvature value (K_u) was calculated considering the strain value ε_{cc} as stated in Equation 2. The calculated curvature was assumed to be uniformly distributed along the plastic hinging height ($0.5h$) as stated in TEC07. Additionally, the curvature distribution was assumed linear outside the plastic moment region and this distribution was taken into account in the calculations (Figure 7). In the calculations, the curvatures were integrated along the column height and as shown in Equation 5, thus the yield and the probable ultimate deflection values were calculated.

$$\Delta_u = \Delta_y + \Delta_p = \frac{\kappa_y L^2}{3} + \left(\kappa_u - \kappa_y\right) L_p \left(L - \frac{L_p}{2}\right) \tag{5}$$

In the analyses, for FRP confined columns, bilinear lateral load (P) – deflection (Δ) graphs were obtained and compared by the experimental data (Figure 3-5). In the analyses of reference columns (S-L-0-00, S-H-0-00 and R-NC-0-00), instead of the FRP confined concrete model, the unconfined concrete and steel models described in TEC07 were used. In this study, since the FRP confined concrete was the major investigation subject, the results related to unconfined concrete are not presented in Table 2.

The comparison of the experimental results with the estimations of the TEC07 indicated that, while the column drift capacity (DR_u) calculated for the FRP confined columns does not exceed 1% (20 mm), the experimental results showed that the columns could attain drift ratios of at least two times the ratios found by the code as can be seen in Table 1. In flexure dominated columns, the components that constitute the tip deflection can be classified as

elastic bending, plastic rotation developing at column ends, shear and bond slip motivated deflections. Since the tip deflection can only be comprised of elastic bending and plastic rotation motivated deflections according to TEC07, the other factors were ignored. Besides, the TEC07 assumption of plastic hinge length being *0.5h* appears to be considerably safe [1, 3]. Similarly, taking the FRP ultimate strain value as half of the value given by the manufacturer or 0.004 leads to over safe designs.

Table 2. The analytical results for the test specimens

Specimen	K_y	M_y	M_y/EI_{cr}	K_u	M_u	Δ_y	P_y	Δ_u	P_u
	rad/km	*kN·m*	*rad/km*	*rad/km*	*kN·m*	*mm*	*kN*	*mm*	*kN*
S-L-1-00	9.79	124.61	7.24	24.65	140.94	9.65	62.31	15.48	70.47
S-L-1-34	11.59	116.10	6.86	23.38	122.62	9.14	58.05	14.67	61.31
S-L-2-00	13.07	110.26	6.58	34.82	115.74	8.77	55.13	18.23	57.87
S-L-2-32	10.83	120.22	7.06	34.22	133.24	9.42	60.11	18.51	66.62
S-H-1-00	9.86	151.92	8.67	23.54	169.13	11.56	75.96	16.54	84.57
S-HC-1-00	9.48	153.92	8.38	21.35	173.14	11.17	76.96	15.51	86.57
R-HC-1-16P	10.78	96.57	7.81	31.55	101.13	10.41	48.29	18.36	50.57
R-MC-1-8P	10.81	97.21	7.67	22.36	100.53	10.23	48.61	15.14	50.27
R-MC-1-NP	11.14	92.23	7.86	23.79	95.00	10.48	46.12	15.81	47.50
R-MC-1-16P	10.04	113.88	7.52	26.12	121.14	10.02	56.94	16.25	60.57

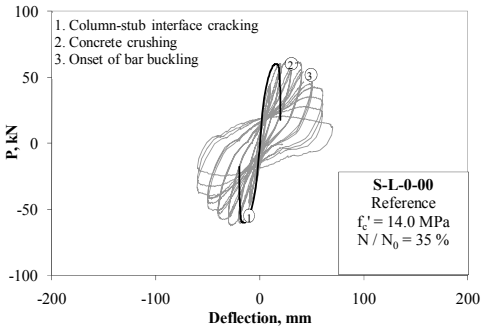

Figure 3. Comparison graphs for the 1st series columns (Cont'd)

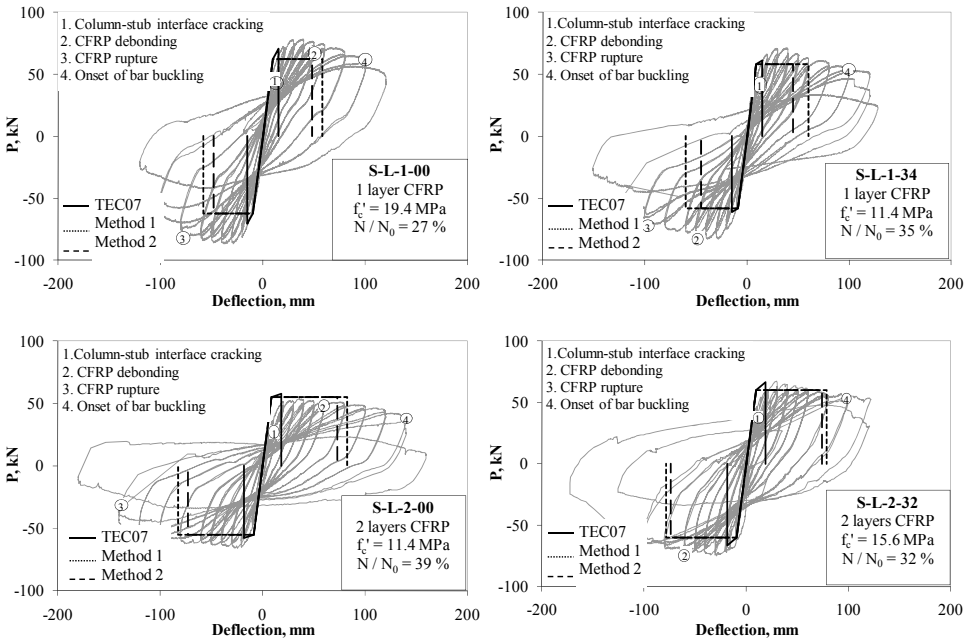

Figure 3. Comparison graphs for the 1st series columns

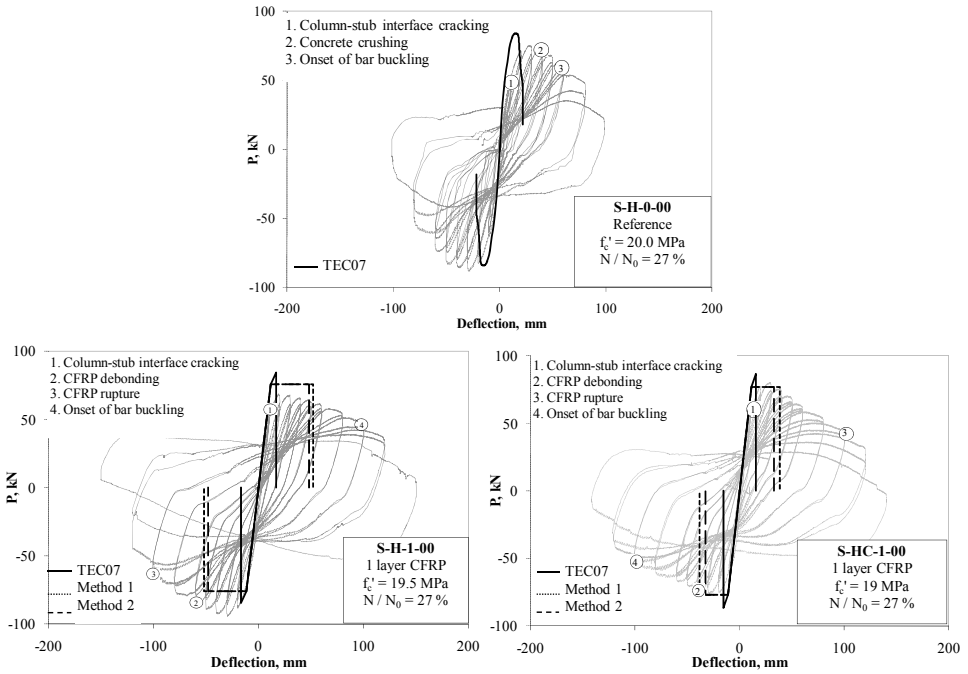

Figure 4. Comparison graphs for the 2nd series columns

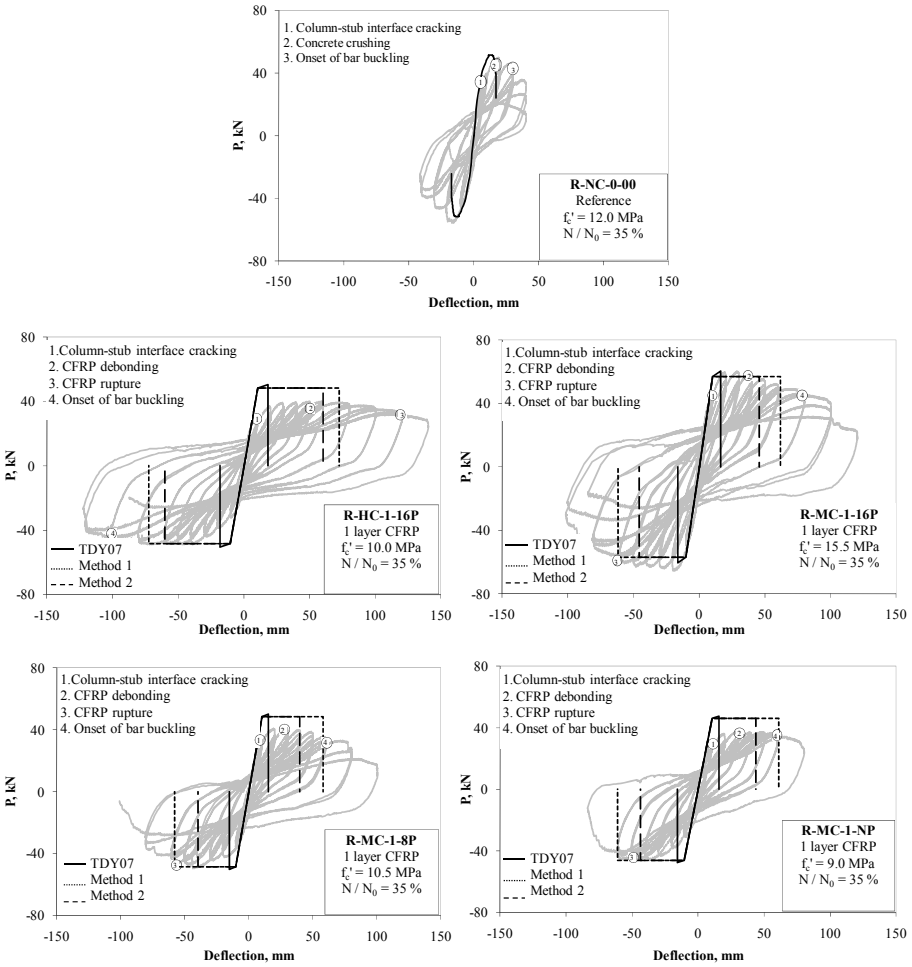

Figure 5. Comparison graphs for the 3rd series columns

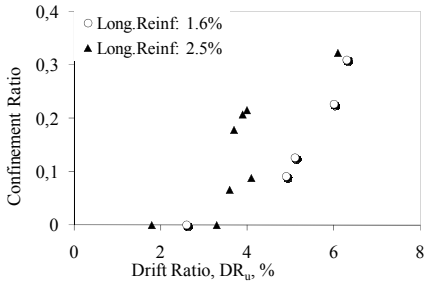

Figure 6. Confinement ratio – Column drift ratio relationship for different longitudinal reinforcement ratios

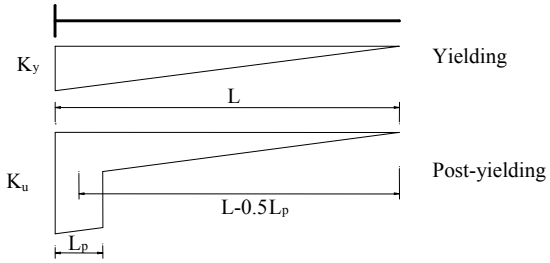

Figure 7. Curvature distribution for the cases of column yield and ultimate limit states

4. PROPOSED DESIGN METHODS

4.1. Method 1: Column Drift Based Design

Eighteen FRP confined column specimens failing in flexure that were tested elsewhere were added to expand the test database and a simplified drift based design method was developed considering the parameters of FRP confinement ratio (ϕ), axial load ratio (n) and longitudinal reinforcement ratio (ρ). The drift capacities (DR_u) were estimated to be linked with these three parameters by using nonlinear regression analysis. The experimental column drift capacity was considered as the drift ratio at which the experimental column lateral strength dropped to 80 percent of its ultimate value. The exponential function that was obtained as a result of the regression analysis and given in Equation 6a had the best agreement with the experimental data (Figure 8a). This equation could not provide sufficient safety considering design regulations since it gives a best estimate for the average value of the tests. It is, therefore, necessary to develop an approach that may be used in design safely. As a result of a series of analyses by using all data in the database, Equation 6b was obtained that can safely predict all experimental data while being economical.

$$DR_u = 2.47 + 50\frac{\phi^{0.64}}{n^{1.29}\rho^{0.35}} \tag{6a}$$

$$DR_u = 2 + 4.5\frac{\phi}{n\rho} \tag{6b}$$

In these equations the values of ϕ, n and ρ are defined in percentiles. The comparisons of analytical drift ratios obtained by this equation with experimental results are given in Figure 8b.It is clear that Equation 6b is a design formula that yields safe results in all circumstances. The numerical comparison of the data in Figure 8 is presented separately in Tables 3a and 3b. As can be observed in these tables, while the standard deviation of the results obtained by Equation 6a from the experimental results is in the range of ±30%, the results obtained by Equation 6b are consistently safe, remaining below the experimental data. While the safety margin sometimes reaches up to 70%, it yields an unsafe result of 5% only for the test carried out by Memon et al. in 2002. The comparison between the design which was obtained by the Method 1 and the experimental lateral load – lateral deflection

envelopes is shown in Figures 3-5. As can be seen in these figures, the proposed column drift based design method represents the effect of FRP confinement safely and can easily be implemented in design. For FRP confined columns, the column drift capacities (DR_u) that were predicted by Method 1 approximately correspond to the ultimate drift ratio at which the column could undergo three stable cycles. These results prove that Method 1 as a design method can be employed safely. The complexity of the FRP design method denoted in TEC07 was simplified by the proposed drift based design method.

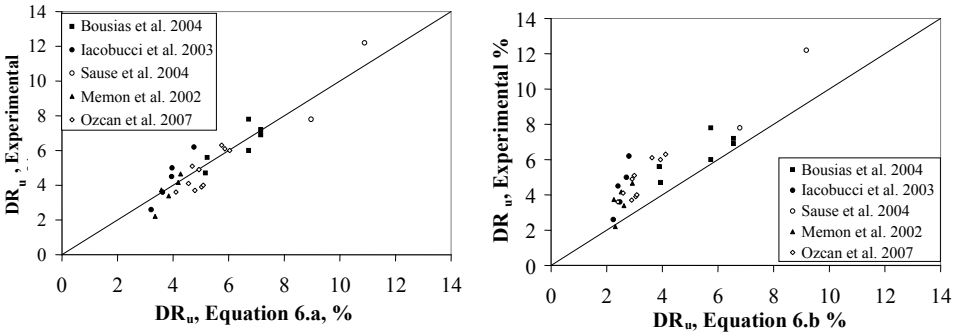

(a) (b)

Figure 8. Method 1: (a) best correlation and (b) the comparison of design equation with the experimental data

4.2. Method 2: Strain Based Design

In the second method, the ultimate strain at the utmost fiber in FRP confined concrete section was calibrated by using the experimental column drift ratios. The main three parameters in Method 1 and previously stated FRP confined column database of 28 columns were also used in this method. Firstly, the yield moment values (M_y) were determined for all the columns in the database by using rectangular stress block and elasto-plastic steel model with standard section analysis. In the next step, column yield moments were divided into cracked concrete rigidity and yield curvatures (K_y) were obtained. The experimental drift ratios for all columns were converted into ultimate lateral deflection (Δ_u) and yield deflection (Δ_y). The plastic hinge length was assumed to be the longer dimension of the column section (h). The reliability of this assumption as opposed to the $0.5h$ value given in TEC07 can be justified based on the results of this experimental study and various tests carried out in the literature [14-16]. Afterwards, the ultimate curvatures (K_u) consistent with the experimental ultimate deflections were calculated using Equation 5. For all columns in the database, the ultimate strain of FRP confined concrete (ε_{cc}) was evaluated by using rectangular stress block and elasto-plastic steel model (Tables 4a, b). The strain values obtained this way were used in a nonlinear regression analysis where the three parameters (FRP confinement ratio (ϕ), axial load ratio (n) and longitudinal reinforcement ratio (ρ) were the independent parameters (Equation 7a). At the end of these analyses, the ultimate concrete strains that yield the best fit for experimental ultimate lateral deflections was determined. Similar to Equation 6a, Equation 7a could not provide sufficient safety for design purposes since it gives the best estimate for the average values of the tests. Thus, Equation 7b was obtained which can predict all experimental results safely and provides the

condition that unconfined ultimate strain is 0.004 for unconfined concrete The calculated $\varepsilon_{cc,p}$ values are provided in Table 4a.

$$\varepsilon_{cc} = 0.019 + 0.418\frac{\phi}{\sqrt{n\rho}} \tag{7a}$$

$$\varepsilon_{cc} = 0.004 + 3.6\frac{\phi}{n\rho} \tag{7b}$$

In Figures 9a and b, the comparisons of the experimentally obtained strain values with those obtained by using the proposed design equations are presented. The comparisons between lateral loads – deflection envelopes that were obtained by Method 2 and experimental results are also shown in Figure 3-5. As can be observed, Method 2 predicts ultimate drift ratios with a slightly higher safety margin compared to Method 1. However, Method 2 permits rather more economical designs when compared with TEC07 design regulations. In the second approach (Method 2), the concrete and steel models stated in the code were further simplified. A rectangular stress block was used for the concrete in compression along with the elasto-plastic steel model. It can be observed that Method 1 predictions of ultimate lateral displacement correspond to displacements at which three stable cycles of displacement excursions did not result in significant lateral strength drop. Furthermore, similar to Method 1, the FRP confinement ratio, the axial load ratio and the longitudinal reinforcement ratio are included to determine the seismic performance of FRP confined columns. In short, in order to determine the column displacement performance limits for the design of FRP confined concrete, a strain based methodology similar to the current TEC07 approach is tailored.

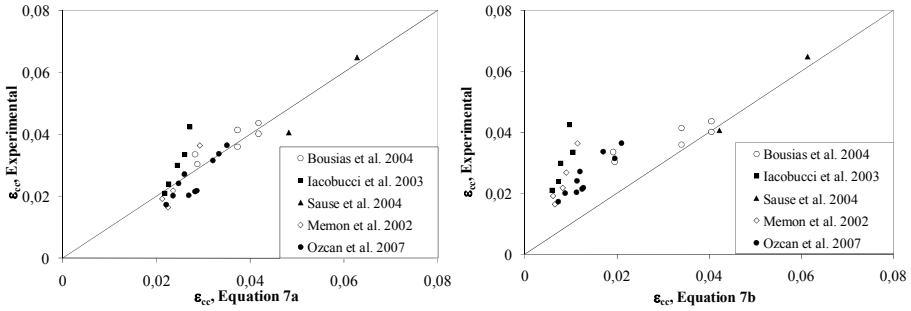

(a) (b)

Figure 9. Method 2: (a) Best correlation and (b) The comparison of design equation with the experimental data

4.3. Recommendations for TEC07 for FRP Retrofit Design

The complicated material models specified in TEC07 are far from being adequate in estimating the inelastic behavior of FRP confined columns. In addition, the column deflections obtained by integrating the curvature distribution using these models are usually

on the excessively safe side. In this study, it was shown that safe and more economical designs could be obtained for FRP confined columns in the light of two different design methods based on column drift ratio and concrete strain. While the design method based on column drift ratio is simpler, the second method, being compatible with the current code regulations, provides a more detailed perspective. Both methods allow the users to estimate the column drift ratio for FRP confined columns or the required FRP confinement amount for a target column drift demand. In the case of Method 1, the required FRP confinement amount for a given column drift demand or column drift capacity of FRP confined column can be determined by using Equations 6a and 6b. For the second method, since a standard section analysis is needed, the material models were simplified (using rectangular stress block for concrete, elasto-plastic steel model and equal yield and ultimate moments). The authors consider that plastic hinge length should be taken as the section dimension in the direction of bending in the calculation of lateral deflections. This dimension is the section diameter for circular columns and section height for square columns; it should be used as the longer dimension of the section for the columns with rectangular sections. For FRP confined concrete, FRP design can be carried out using Equation 7b. In order to determine the damage limits in the current code, the strain limits are required. For both methods proposed in this study, the collapse prevention limit (CP) may be taken as the column drift capacity (DR_u). In a similar manner75 percent of DR_u may be taken as the life safety limit, (LS). The transition point that corresponds to the yield deflection of the column, on the other hand, may be used to represent the immediate occupancy (IO) performance limit. The design example presented in appendix is believed to shed light on the numerical application of the design methods. As can be seen in the example design, the current TEC07 regulations do not provide economical solutions; and, therefore, discourage the use of FRPs in retrofit designs. The methodologies proposed in this study, however, have shown analytically and experimentally that economical FRP retrofitting is possible and the designs attained this way provide sound alternatives to classical column retrofit methodologies available in the literature.

5. RESULTS

In this study, the ability of TEC07 design equations to estimate the load-deformation response of the tests conducted at METU was investigated experimentally and analytically. It was found that estimations made by TEC07 are excessively safe and uneconomical for the FRP confinement implementations. Current code regulations unnecessarily augment the FRP amount to achieve the required ductility level and therefore discourage retrofitting of columns using FRPs in Turkey. In the final stages of this work, in addition to the data generated in the experimental phase of this study, the data assembled from the literature was used to form a sound database. Based on this database, two different design methods were developed. The first design method is based on column drift ratio. In this method, the column drift ratios were expressed as a function of three parameters to render a direct solution for FRP design. The second is a method based on ultimate concrete strain limit, the column drift ratios were evaluated by integrating elastic and plastic curvatures. In this proposed design technique the rectangular stress block and the elasto-plastic steel model were used in view of their simplicity. It was proved that both methods can be used in the FRP retrofit design of columns effectively and provide economical design solutions without sacrificing structural safety

Table 3a. The results of Method 1 (on the data from the literature)

Research	b	h	L	r	f_{cm}	A_s	f_y	E_f	ε_{fu}	t_j	κ_a	ρ	n	ϕ	DR_u	Equation 6a		Equation 6b	
																$DR_{u,p}$	DR_u / $DR_{u,p}$	$DR_{u,p}$	DR_u / $DR_{u,p}$
	mm	*mm*	*mm*	*mm*	*MPa*	mm^2	*MPa*	*MPa*		*mm*			*%*		*%*	*%*		*%*	
Bousias et al. [2]	250	500	1600	30	18.1	1017.9	559.5	230000	0.015	0.26	0.387	0.81	34	0.115	5.6	5.23	1.07	3.90	1.44
	250	500	1600	30	16.7	1017.9	559.5	230000	0.015	0.26	0.387	0.81	36	0.125	4.7	5.16	0.91	3.94	1.19
	250	500	1600	30	17.9	1017.9	559.5	230000	0.015	0.65	0.387	0.81	35	0.291	6.9	7.15	0.96	6.56	1.05
	500	250	1600	30	17.9	1017.9	559.5	230000	0.015	0.65	0.387	0.81	35	0.291	7.2	7.15	1.01	6.56	1.10
	250	500	1600	30	18.7	1017.9	559.5	70000	0.031	0.85	0.387	0.81	34	0.229	6.0	6.72	0.89	5.75	1.04
	500	250	1600	30	18.7	1017.9	559.5	70000	0.031	0.85	0.387	0.81	34	0.229	7.8	6.72	1.16	5.75	1.36
Iacobucci et al. [3]	305	305	1473	16	36.5	2513.3	465	76350	0.013	1.00	0.466	2.70	33	0.081	4.5	3.94	1.14	2.41	1.87
	305	305	1473	16	36.9	2513.3	465	76350	0.013	2.00	0.466	2.70	56	0.159	3.6	3.62	0.99	2.47	1.46
	305	305	1473	16	36.9	2513.3	465	76350	0.013	1.00	0.466	2.70	56	0.080	2.6	3.21	0.81	2.24	1.16
	305	305	1473	16	37.0	2513.3	465	76350	0.013	3.00	0.466	2.70	56	0.238	5.0	3.96	1.26	2.71	1.85
	305	305	1473	16	37.0	2513.3	465	76350	0.013	2.00	0.466	2.70	33	0.159	6.2	4.75	1.31	2.80	2.21
Sause et al.[4]	458	458	2419	45	24.8	3096.6	460	76200	0.015	6.00	0.570	1.48	29	0.688	12.2	10.88	1.12	9.18	1.33
	458	458	2419	45	24.8	3096.6	460	76200	0.015	4.00	0.570	1.48	29	0.459	7.8	8.96	0.87	6.78	1.15
Memon et al. [5]	305	305	1473	16	42.5	2450.4	465	24693	0.023	2.50	0.466	2.63	33	0.101	4.2	4.18	0.99	2.52	1.65
	305	305	1473	16	42.7	2450.4	465	24693	0.023	5.00	0.466	2.63	55	0.201	3.4	3.84	0.88	2.62	1.29
	305	305	1473	16	43.3	2450.4	465	24693	0.023	2.50	0.466	2.63	55	0.099	2.2	3.35	0.66	2.31	0.95
	305	305	1473	16	43.7	2450.4	465	24693	0.023	1.25	0.466	2.63	32	0.049	3.7	3.58	1.04	2.26	1.65
	305	305	1473	16	44.2	2450.4	465	24693	0.023	7.50	0.466	2.63	54	0.292	4.7	4.27	1.09	2.92	1.59

Table 3b. The results for Method 1 (on the data generated in this study)

Research	b	h	L	r	f_{cm}	A_s	f_y	E_f	ε_{fu}	t_j	κ_a	ρ	n	ϕ	DR_u	Equation 6a		Equation 6b	
																$DR_{u,p}$	DR_u / $DR_{u,p}$	$DR_{u,p}$	DR_u / $DR_{u,p}$
	mm	*mm*	*mm*	*mm*	*MPa*	mm^2	*MPa*	*MPa*		*mm*			*%*		*%*	*%*		*%*	
Ozcan et al. [1,14-16]	350	350	2000	30	19.4	2035.8	287	230000	0.015	0.165	0.542	1.66	27	0.091	4.9	4.93	0.99	2.92	1.68
	350	350	2000	30	14.0	2035.8	287	230000	0.015	0.165	0.542	1.66	34	0.126	5.1	4.69	1.09	3.00	1.70
	350	350	2000	30	11.4	2035.8	287	230000	0.015	0.33	0.542	1.66	40	0.309	6.3	5.75	1.10	4.12	1.53
	350	350	2000	30	15.6	2035.8	287	230000	0.015	0.33	0.542	1.66	32	0.226	6.0	6.04	0.99	3.93	1.53
	350	350	2000	30	20.0	3041.1	287	230000	0.015	0.165	0.542	2.48	27	0.088	4.1	4.56	0.90	2.59	1.58
	350	350	2000	10	22.0	3041.1	287	230000	0.015	0.165	0.407	2.48	27	0.060	3.6	4.10	0.88	2.40	1.50
	200	400	2000	30	10.0	2035.8	287	230000	0.015	0.165	0.755	2.54	35	0.322	6.1	5.86	1.04	3.63	1.68
	200	400	2000	30	10.5	2035.8	287	230000	0.015	0.165	0.437	2.54	35	0.178	3.7	4.79	0.77	2.90	1.28
	200	400	2000	30	9.0	2035.8	287	230000	0.015	0.165	0.437	2.54	35	0.207	3.9	5.03	0.78	3.05	1.28
	200	400	2000	30	15.0	2035.8	287	230000	0.015	0.165	0.755	2.54	35	0.215	4.0	5.09	0.79	3.09	1.30

Table 4a. The results for Method 2 (on the data from the literature)

Research	Column	b	h	L	r	f_{cm}	A_s	f_y	E_f	ε_{fu}	t_j	κ_a	ρ	n	ϕ	ε_{cc}	Eq.7a	$\varepsilon_{cc,p}$ / ε_{cc}
		mm	*mm*	*mm*	*mm*	*MPa*	*mm²*	*MPa*	*MPa*				*%*	*%*			$\varepsilon_{cc,p}$	
Bousias et al. [2]	US-C2	250	500	1600	30	18.1	1017.9	559.5	230000	0.015	0.26	0.387	0.81	34	0.115	0.03358	0.0282	0.84
	US-C2in	250	500	1600	30	16.7	1017.9	559.5	230000	0.015	0.26	0.387	0.81	36	0.125	0.03041	0.0287	0.94
	US-C5	250	500	1600	30	17.9	1017.9	559.5	230000	0.015	0.65	0.387	0.81	35	0.291	0.04372	0.0417	0.95
	UW-C5	500	250	1600	30	17.9	1017.9	559.5	230000	0.015	0.65	0.387	0.81	35	0.291	0.04020	0.0417	1.04
	US-G5	250	500	1600	30	18.7	1017.9	559.5	70000	0.031	0.85	0.387	0.81	34	0.229	0.03601	0.0373	1.03
	UW-G5	500	250	1600	30	18.7	1017.9	559.5	70000	0.031	0.85	0.387	0.81	34	0.229	0.04143	0.0373	0.90
Iacobucci et al. [3]	ASC-2NS	305	305	1473	16	36.5	2513.3	465	76350	0.013	1.00	0.466	2.70	33	0.081	0.02397	0.0226	0.94
	ASC-3NS	305	305	1473	16	36.9	2513.3	465	76350	0.013	2.00	0.466	2.70	56	0.159	0.02996	0.0244	0.81
	ASC-4NS	305	305	1473	16	36.9	2513.3	465	76350	0.013	1.00	0.466	2.70	56	0.080	0.02098	0.0217	1.03
	ASC-5NS	305	305	1473	16	37.0	2513.3	465	76350	0.013	3.00	0.466	2.70	56	0.238	0.04251	0.0271	0.64
	ASC-6NS	305	305	1473	16	37.0	2513.3	465	76350	0.013	2.00	0.466	2.70	33	0.159	0.03349	0.0260	0.78
Sause et al. [4]	F1	458	458	2419	45	24.8	3096.6	460	76200	0.015	6.00	0.570	1.48	29	0.688	0.06485	0.0628	0.97
	F2	458	458	2419	45	24.8	3096.6	460	76200	0.015	4.00	0.570	1.48	29	0.459	0.04063	0.0482	1.19
Memon et al. [5]	ASG-2NSS	305	305	1473	16	42.5	2450.4	465	24693	0.023	2.50	0.466	2.63	33	0.101	0.02183	0.0235	1.08
	ASG-3NSS	305	305	1473	16	42.7	2450.4	465	24693	0.023	5.00	0.466	2.63	55	0.201	0.02686	0.0260	0.97
	ASG-4NSS	305	305	1473	16	43.3	2450.4	465	24693	0.023	2.50	0.466	2.63	55	0.099	0.01642	0.0225	1.37
	ASG-5NSS	305	305	1473	16	43.7	2450.4	465	24693	0.023	1.25	0.466	2.63	32	0.049	0.01918	0.0212	1.11
	ASG-6NSS	305	305	1473	16	44.2	2450.4	465	24693	0.023	7.50	0.466	2.63	54	0.292	0.03645	0.0292	0.80

Table 4b. The results for Method 2 (on the data generated in this study)

Research	Column	b	h	L	r	f_{cm}	A_s	f_y	E_f	ε_{fu}	t_j	κ_a	ρ	n	ϕ	ε_{cc}	Eq.7a	$\varepsilon_{cc,p}$ / ε_{cc}
		mm	*mm*	*mm*	*mm*	*MPa*	*mm²*	*MPa*	*MPa*				*%*	*%*			$\varepsilon_{cc,p}$	
Ozcan et al. [1,14-16]	S-L-1-00	350	350	2000	30	19.4	2035.8	287	230000	0.015	0.165	0.542	1.66	27	0.091	0.02419	0.0247	1.02
	S-L-1-34	350	350	2000	30	14.0	2035.8	287	230000	0.015	0.165	0.542	1.66	34	0.126	0.02721	0.0260	0.95
	S-L-2-00	350	350	2000	30	11.4	2035.8	287	230000	0.015	0.33	0.542	1.66	40	0.309	0.03649	0.0350	0.96
	S-L-2-32	350	350	2000	30	15.6	2035.8	287	230000	0.015	0.33	0.542	1.66	32	0.226	0.03153	0.0320	1.02
	S-H-1-00	350	350	2000	30	20.0	3041.1	287	230000	0.015	0.165	0.542	2.48	27	0.088	0.02015	0.0235	1.17
	S-HC-1-00	350	350	2000	10	22.0	3041.1	287	230000	0.015	0.165	0.407	2.48	27	0.060	0.01730	0.0221	1.28
	R-HC-1-16P	200	400	2000	30	10.0	2035.8	287	230000	0.015	0.165	0.755	2.54	35	0.322	0.03380	0.0333	0.98
	R-MC-1-8P	200	400	2000	30	10.5	2035.8	287	230000	0.015	0.165	0.437	2.54	35	0.178	0.02037	0.0269	1.32
	R-MC-1-NP	200	400	2000	30	9.0	2035.8	287	230000	0.015	0.165	0.437	2.54	35	0.207	0.02154	0.0282	1.31
	R-MC1-16P	200	400	2000	30	15.0	2035.8	287	230000	0.015	0.165	0.755	2.54	35	0.215	0.02188	0.0285	1.30

6. APPENDIX: DESIGN EXAMPLE – METHOD 1 AND 2

In this design example, the FRP confinement design for the test specimen S-L-1-00 that was tested in METU by applying proposed design methods is presented. Here, the drift demand of the unconfined column was determined according to TEC07 by using a single degree of freedom column model. The drift demand of the column was determined by using the design spectrum for assumed soil conditions and the calculation steps that are related to FRP confinement are presented below. The converted spectral acceleration and deflection values for unconfined column are shown in Figure 10.

Column Properties:

- Cross sectional dimensions of the column: 350 × 350
- Column height: 2000 mm
- f_c=20 MPa, Clear cover: 30 mm
- Corner rounding radius: 30 mm
- Axial load: N=700 kN,
- By standard section analysis:
  Column yield load: 70.6 kN, yield curvature: 9.8×10^{-6} rad/mm
- Longitudinal reinforcement: 8ϕ18 mm
- Transverse reinforcement: ϕ10/200 mm
- f_y=287 MPa, ε_{su}=0.05, ε_{sy}=0.001435 (Elasto-plastic)
- Soil conditions: Z2, T_A=0.15s, T_B=0.4s

$$m = \frac{700\text{kN}}{9.81\text{m/s}^2} = 71.36\text{kNs}^2/\text{m} \text{ (Axial load compatible mass)}$$

$$I_{cr} = 0.613I = 0.613\left(\frac{350^4}{12}\right) = 767.0\times10^6\,\text{mm}^4 \text{ (Cracked moment of inertia)}$$

$$k = \frac{3EI_{cr}}{L^3} = \frac{3\times28000\times767\times10^6}{2000^3} = 8053.5\text{kN/m}$$

$$T = 2\pi\sqrt{\frac{m}{k}} = 2\pi\sqrt{\frac{71.36}{8053.5}} = 0.59\text{s}, w^2 = \frac{k}{m} = 112.9\text{s}^{-2} \rightarrow w = 10.6\text{s}^{-1}$$

$$S_{De} = \frac{S_{ae}}{w^2} = \frac{0.73\times9.81}{112.9} = 63.4\text{mm}$$

$$a_y = \frac{70.6\text{kN}}{700\text{kN}} = 0.101 \text{ (acceleration coefficient at yielding)}$$

$$R_y = \frac{S_{ae}}{a_y} = \frac{1}{0.101} = 9.92$$

$$C_{R1} = 1(T > T_B)$$

$$S_d = C_{R1}S_{De} = 1\times63.1 = 63.4\text{mm} \approx 65\text{mm} \rightarrow DR_u \approx 3.25\%$$

As can be seen above, for a column of 2.0 meters in height S_d = 65.0 mm corresponds to a drift demand of 3.25 percent. The values are presented graphically in Figure 10. The layer number of FRP that provides calculated drift ratio will be determined by standard section analysis as stated below. In the calculations, rectangular stress block and elasto-plastic steel model was used.

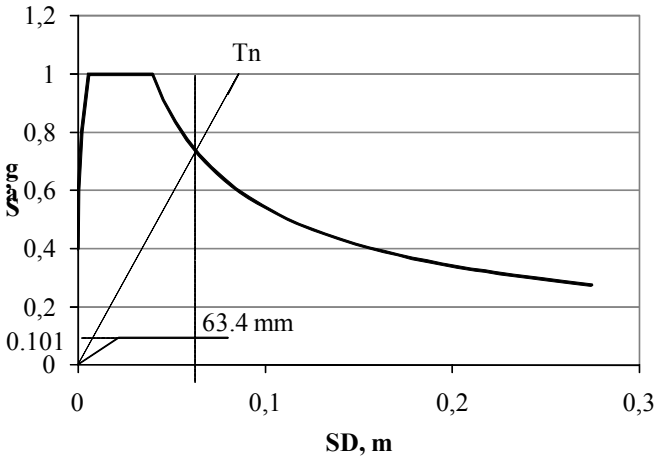

Figure 10. The determination of spectral acceleration and displacement for sample design column

Design according to current code

$$\Delta_u = \frac{\kappa_y L^2}{3} + \left(\kappa_u - \kappa_y\right) L_p \left(h - \frac{L_p}{2}\right)$$

$$\Delta_u = \frac{9.8\times10^{-6}\times2000^2}{3} + \left(\kappa_u - 9.8\times10^{-6}\right)\frac{350}{2}\left(2000 - \frac{350}{4}\right) = 65\text{mm}$$

$\kappa_u = 165.0\text{rad/km} \rightarrow \varepsilon_{cc} = 0.024$ (Yield and ultimate states were calcualated by section analysis)

$$\varepsilon_{cc} = 0.002\left(1 + 15\left(\frac{f_l}{f_c}\right)^{0.75}\right) = 0.002\left(1 + 15\left(\frac{f_l}{20}\right)^{0.75}\right) = 0.024 \rightarrow f_l = 25.24\text{MPa}$$

$$f_l = \frac{\left(b+h\right)E_j\varepsilon_f t_j}{bh}\kappa_a = \frac{\left(350+350\right)230000\times0.015\times t_j}{350\times350}.\left(1 - \frac{2\left(350-2\times30\right)^2}{3\times350^2}\right) = 25.24\text{MPa}$$

$$t_j = 2.36\text{mm} \rightarrow \frac{2.36}{0.165} = 14.3 = 15\text{layers (FRP thickness was used as 0.165 mm)}$$

As can be clearly observed, the design performed according to de current code is found to be over safe and uneconomical.

Design according to Method 1

$$DR_u = 2 + 4.5\frac{\phi}{n\rho} = 2 + 4.5\frac{\phi}{26\times 1.66} = 3.25 \rightarrow \phi = 0.120$$

$$\phi = \frac{(b+h)E_j\varepsilon_f t_j}{bhf_c'}\kappa_a = \frac{(350+350)230000\times 0.015\times t_j}{350\times 350\times 20}.\left(1-\frac{2(350-2\times 30)^2}{3\times 350^2}\right) = 0.120$$

$$t_j = 0.224\text{mm} \rightarrow \frac{0.224}{0.165} = 1.35 = 2\text{layers}$$

Design according to Method 2

$\kappa_y = 10\text{rad/km}$ (Using rectangular stress block and elasto-plastic steel model)

$$\Delta_u = 65\text{mm} = \kappa_y\frac{L^2}{3} + (\kappa_u - \kappa_y)L_p\left(L - \frac{L_p}{2}\right), L_p = h = 350\text{mm}$$

$$65 = 10\times 10^{-6}\times\frac{2000^2}{3} + (\kappa_u - 10)\times 10^{-6}\times 350\times\left(2000 - \frac{350}{2}\right) \rightarrow \kappa_u \simeq 90.9\text{rad/km}$$

$$\frac{\varepsilon_{cc}}{c} = \frac{\varepsilon_{s1}}{c-cc} = \frac{\varepsilon_{s2}}{h/2-c} = \frac{\varepsilon_{s3}}{h-c-cc}$$ (cc: clear cover)

$$N = 0.85f_c'0.85cb_w + A_{s1}f_{s1} + A_{s2}f_{s2} - A_{s3}f_{s3}$$

$$0.85^2\times 20c\times 350 + 3\pi 9^2\times 287 - 2\pi 9^2\times 90.9\times 10^{-6}\times(175-c)2\times 10^5 - 3\pi 9^2\times 287 = 700000\text{N}$$

$$c = 162.1\text{mm} \rightarrow \varepsilon_{cc} = \kappa_u.c = 90.9\times 10^{-6}\times 162.1 = 0.0147$$

$$\frac{0.0147}{162.1} = \frac{\varepsilon_{s1}}{162.1-30} = \frac{\varepsilon_{s2}}{350/2-162.1} = \frac{\varepsilon_{s3}}{350-162.1-30}$$

$$\left.\begin{array}{l}\varepsilon_{s1} = 0.0120\\ \varepsilon_{s2} = 0.00117\\ \varepsilon_{s3} = 0.0143\end{array}\right\}\text{All longitudinal reinforcement yielded except the midbars}$$

Since the calculated concrete strain will be provided by FRP confinement, if the $\phi/n\rho$ ratio will be determined the following results are obtained.

$$\varepsilon_{cc} = 0.004 + 3.6\frac{\phi}{n\rho} = 0.004 + 3.6\frac{\phi}{26\times 1.66} = 0.0147 \rightarrow \phi = 0.128$$

$$\phi = \frac{(b+h)E_j\varepsilon_f t_j}{bhf_c'}\kappa_a = \frac{(350+350)230000\times 0.015\times t_j}{350\times 350\times 20}.\left(1-\frac{2(350-2\times 30)^2}{3\times 350^2}\right) = 0.128$$

$$t_j = 0.239mm \rightarrow \frac{0.239}{0.165} = 1.45 = 2layers$$

As can be seen, both methods provide approximately 7 times more economical FRP designs according to the current code.

Index

***b, h, L, r*:** Column width, length, height and corner rounding radius

cc = clear cover

***f_{cm}, f_{cc}*:** Unconfined and confined concrete strength

***f_l*:** Lateral pressure of FRP

***ε_{cc}, $\varepsilon_{cc,p}$*:** FRP confined concrete ultimate strain and design value

***κ_a*:** Shape efficiency coefficient of FRP

***ρ, ρ_f*:** Longitudinal reinforcement ratio and FRP volumetric ratio

***ε_f, ε_{fu}*:** FRP strain and ultimate FRP strain

***E_f*:** FRP elasticity modulus

***ϕ*:** FRP confinement ratio

***DR, DR_u*:** Drift ratio and ultimate drift ratio

***$DR_{u,p}$*:** Design ultimate drift ratio

***A_s*:** Area of longitudinal reinforcement

***n*:** Axial load ratio

***EI_{cr}*:** Cracked section rigidity

***Δ_y, Δ_u, F_y, F_u*:** Deflection and lateral loads for yield and ultimate states

***K_y, K_u, M_y, M_u*:** Curvature and moments for yield and ultimate states

***Δ_p, L_p*:** Plastic deflection and plastic hinge length

***t_j*:** FRP thickness

References

[1] Ozcan, O., Binici, B., Ozcebe, G., Improving Seismic Performance of Deficient Reinforced Concrete Columns using Carbon Fiber-Reinforced Polymers. Engineering Structures, 30, 1632-1646, 2008.

[2] Bousias, S.N., Triantafilluo, T.C., Fardis, M.N., Spathis, L., O'Regan, B.A., Fiber-Reinforced Polymer Retrofitting of Rectangular Reinforced Concrete Columns with or without Corrosion, ACI Structural Journal, 101(4), 512-520, 2004.

[3] Iacobucci, R.D., Sheikh, S.A., Bayrak, O., Retrofit of Square Concrete Columns with Carbon Fiber-Reinforced Polymer for Seismic Resistance, ACI Structural Journal, 100(6), 785-794, 2003.

[4] Sause, R., Harries, K.A., Walkup, S.L., Pessiki, S., Ricles, J.M., Flexural Behavior of Concrete Columns Retrofitted with Carbon Fiber Reinforced Polymer Jackets, ACI Structural Journal, 101(5), 708-716, 2004.

[5] Memon, M.S., Sheikh, S.A., Seismic Behavior of Square Concrete Columns Retrofitted with Glass Fibre-Reinforced Polymers, Research Report, Dept. Of Civil Engineering, University of Toronto, 2002.

[6] Seible F., Priestley M.J.N., Hegemier G.A., Innamorato D., Seismic Retrofitting of RC Columns with Continuous Carbon Fiber Jackets. Journal of Composites for Construction, 1(2), 52-62, 1997.

[7] Sheikh SA, Yau G. Seismic Behavior of Concrete Columns Confined with Steel and Fiber-Reinforced Polymers, ACI Structural Journal, 99(1), 72-80, 2002.

[8] Xiao Y, Ma R. Seismic Retrofit of RC Circular Columns Using Prefabricated Composite Jacketing, Journal of Structural Engineering, 123(10), 1356-1364, 1997.

[9] Saadatmanesh H, Ehsani MR, Li MW. Strength and Ductility of Concrete Columns Externally Reinforced with Fiber Composite Straps, ACI Structural Journal, 91(4), 434-447, 1994.

[10] Saadatmanesh H, Ehsani MR, Jin L. Repair of Earthquake - Damaged RC Columns with FRP Wraps. ACI Structural Journal, 94(2), 206–15, 1997.

[11] TEC 2007, "Deprem Bölgelerinde Yapılacak Binalar Hakkındaki Yönetmelik", Bayındırlık ve İskan Bakanlığı, 2007.

[12] İlki A, Peker O, Karamuk E, Demir C, Kumbasar N. FRP Retrofit of Low and Medium Strength Circular and Rectangular Reinforced Concrete Columns, ASCE Journal of Materials in Civil Engineering, 20(2), 169-88, 2008.

[13] İlki A, Peker O, Karamuk E, Demir C, Kumbasar N. Axial Behavior of RC Columns Retrofitted with FRP Composites, Springer, Advances in Earthquake Engineering for Urban Risk Detection, 301-16, 2006.

[14] Ozcan O. Improving Ductility and Shear Capacity of Reinforced Concrete Columns with Carbon Fiber Reinforced Polymer (CFRP), PhD Thesis, 243 sayfa, 2009.

[15] Ozcan O, Binici B, Ozcebe G. Improving Strength and Ductility of Reinforced Concrete Columns using Carbon Fiber Reinforced Polymer (CFRP). In: Ninth Canadian Conference on Earthquake Engineering, Ottawa, ON, June 2007.

[16] Ozcan O, Binici B, Ozcebe G. Seismic Retrofitting of Reinforced Concrete Columns using Carbon Fiber Reinforced Polymer (CFRP), In: Asia-Pacific Conference on FRP in Structures (APFIS 2007), IIFC, Hong Kong, China, December 2007.